JOURNAL OF THEORETICAL
AND APPLIED MECHANICS
47, 3, pp. 617-628, Warsaw 2009

DYNAMIC BEHAVIOR OF BONE-IMPLANT SUBSTITUTE SYSTEMS. NUMERICAL AND EXPERIMENTAL STUDY

Bartosz Nowak
Mariusz Kaczmarek
Józef Kubik

Kazimierz Wielki University in Bydgoszcz, Institute of Environmental Mechanics and Applied Computer Science, Bydgoszcz, Poland
e-mail: bartek@ukw.edu.pl

In this paper, a study of substitute systems of an implanted bone was presented from the point of view of elaboration of a method for diagnosing the state of integrity of the bone-implant attachment based on vibrational techniques. Dynamic parameters of the systems were eshablished as sets of eigenfrequencies/resonance frequencies using numerical procedures and experimental modal analysis. The shifts of values of the parameters were discussed in relation to the loosening of contact between the bone and implant. The numerical and experimental results were compared and their consequences for application of vibrational techniques to real anatomical systems discussed.

Key words: dynamics, biomechanics, bone, implant

1. Introduction

Destructive diseases or accidents call for prosthesis, which nowadays in many aspects have achieved a certain degree of perfection, yielding pain-free functionality and longevity. However, gradual loosening of the implant-bone attachment integrity due to wear, bone regress (related to aging or diseases) and micro mechanical damage leads eventually to failure of the replacement and thus to painful consequences. A repetition of the implanting surgery takes place under unfavorable conditions (Keener and Callaghan, 2003). The total costs of the healing are multiplied taking into account the repetition and recovery issues.

The existing methods of monitoring of quality of implants fixation are based either on the X-ray imaging or ultrasonic inspection. Among mostly used techniques are: standard radiography, contrast radiography and scyntigraphy. In some cases, however, they are impaired by shielding effects (especially when complicated shapes of the prosthesis are needed) and reveal insufficient sensitivity and specificity (Zilkens *et al.*, 1998; Lieberman *et al.*, 1993). The effectiveness of these methods is particularly questioned in early stage of deterioration of bone implant integrity. There is one more disadvantage of the technique that too frequent X-ray irradiation may lead to other serious injures.

An alternative method of diagnosis is considered, based on the monitoring of the integrity of the implant and bone by checking the changes of its vibrational characteristics. Unlike the ultrasonic inspection, which works based on the physical principles of propagation and reflection for waves of certain frequency chosen for the tested tissue, the considered method would rely on monitoring of the shifts of the characteristic frequency caused by the changes in mechanical properties of the system due to the deteriorating state of the implant.

There is a limited number of studies attempting to develop appropriate vibrational techniques to detect changes in bone-implant integrity (Georgiou and Cunningham, 2001; O'niell and Harris, 1984; Phillips and Kattapuram, 1982; Qi *et al.*, 2003; Rosenstein *et al.*, 1989). They generally fall into two categories: numerical studies and experimental tests. Numerical simulations are concentrated on the solution of an eigenproblem. In experimental studies, two main types of excitations are used: harmonic and impulse impact. Even though the vibrational methods show sufficient sensitivity in diagnosing of the late state loosening their effectiveness in an earlier state still suffer the lack of sensitivity.

The aim of this study is to investigate the influence of state of integrity of substitute models of an implanted bone on the spectrum of vibration. Experimental modal analysis and numerical simulations on the basis of the finite element method are performed. The analysis is focused on the comparison of the results and on finding changes of the dynamic characteristics of the systems due to loosening. The usefulness of the vibrational tool in the diagnostic process is discussed.

2. Materials and methods

In the numerical and experimental part of this study, two substitute systems which model the implanted bone are considered. The first system denoted as APB (Aluminium-Pom-C-Brass) consists of three components: a hollowed rod made of aluminum simulating the bone, muff made of Pom-C feigning the layer of bone cement and brass rod modeling the implant. In the second system denoted as PB (Pom-C-Brass) there are: a hollowed rod made of Pom-C which performs like both bone and bone cement, and brass rod modeling the implant.The geometry and components of the numerical models of the substitute systems are given in Fig. 1.

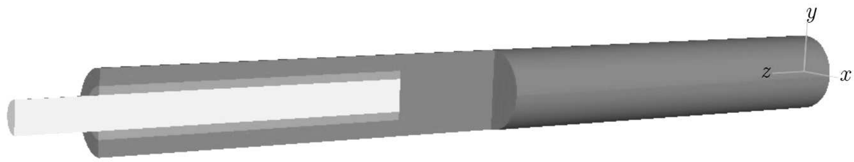

Fig. 1. Geometry of the numerical model of the substitute system

The elastic constants and densities of the three materials used to make the system are presented in Table 1. The mechanical properties of the materials of substitute systems roughly match the parameters of bone, bone cement and implant.

Table 1. Elastic constants and densities of considered materials

Material	v [–]	E [GPa]	ρ [kg/m^3]
Aluminium	0.35	71	2700
Brass	0.30	35	8400
POM-C	0.31	3	1410

The deterioration of bone-implant attachment is modeled as a loss of contact (connection) between the bone and implant. The quantitative measure of drop of the connection can be described by the following expression

$$D = \Big(1 - \frac{A_i}{A_I}\Big)100\% \tag{2.1}$$

where D is the deterioration parameter, A_I describes the initial area of the connected surfaces and A_i describes the current or actual area of connected surfaces.

In the numerical and experimental part of the study, two cases of deterioration are introduced to the systems which are described by values of the parameter D: 25% and 75%, Fig. 2. The substitute system with no loss of contact denoted by $D = 0\%$ served as a referance case.

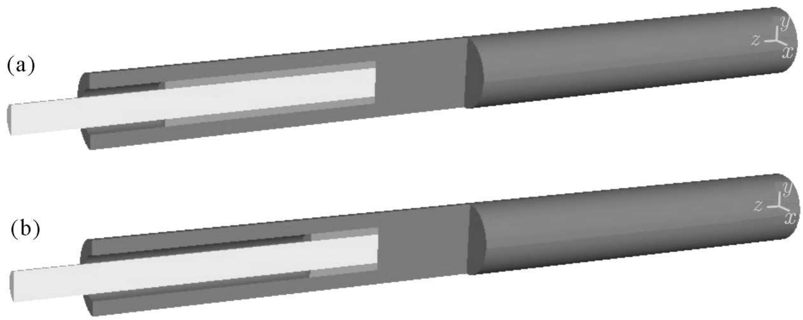

Fig. 2. Geometry of systems with the following deteriorations: (a) $D = 25\%$, (b) $D = 75\%$

In the procedure of eigenvalue/resonance frequency extraction, free-free boundary conditions are applied to the systems, which means lack of external fixation of the system.

2.1. Model and numerical study

The description of dynamics of the considered system is based on the continuum mechanics approach, in which the equation of motion after discretization using finite element method takes the form (Zienkiewicz and Taylor, 2001)

$$\mathsf{M}\ddot{\boldsymbol{U}}(t) + \mathsf{C}\dot{\boldsymbol{U}}(t) + \mathsf{K}\boldsymbol{U}(t) = \boldsymbol{R}(t) \tag{2.2}$$

where M, C, K are mass, damping and stiffness matrices, $\ddot{\boldsymbol{U}}$, $\dot{\boldsymbol{U}}$, $\boldsymbol{U}$ denote acceleration, velocity and displacement vectors, respectively, $\boldsymbol{R}$ is the external load vector and t serves as the time parameter.

The matrices M, C, K have a bandwidth which is determined by the number of degrees of freedom of finite elements in the system. Therefore, the topology of the finite element mesh determines the order and bandwidth of the system matrices. In the following study, the free vibration response of the structure with damping neglected is taken into account, therefore equation (2.2) is reduced to the form

$$\mathsf{M}\ddot{\boldsymbol{U}}(t) + \mathsf{K}\boldsymbol{U}(t) = \mathbf{0} \tag{2.3}$$

The solution is postulated in the form

$$\boldsymbol{U}(t) = \boldsymbol{\phi} \sin \omega t \tag{2.4}$$

which leads to the following formulation of the eigenproblem

$$\mathsf{K}\boldsymbol{\phi} = \omega^2 \mathsf{M} \tag{2.5}$$

The eigenproblem yelds n eigensolutions: $(\omega_1^2, \boldsymbol{\phi}_1), (\omega_1^2, \boldsymbol{\phi}_2), \dots, (\omega_n^2, \boldsymbol{\phi}_n)$, whose eigenvectors are $\mathbf{M}$-orthonormalized

$$\begin{aligned} &\boldsymbol{\phi}_i \mathbf{M} \boldsymbol{\phi}_j = \begin{cases} 1 & \text{for} \quad i = j \\ 0 & \text{for} \quad i \neq j \end{cases} \\ &0 \leqslant \omega_1^2 \leqslant \omega_1^2 \ldots \leqslant \omega_i^2 \ldots \leqslant \omega_n^2 \end{aligned} \tag{2.6}$$

The matrix of eigenvectors is then

$$\boldsymbol{\Phi} = \begin{bmatrix} \boldsymbol{\phi}_1 & \boldsymbol{\phi}_2 & \cdots & \boldsymbol{\phi}_i & \cdots & \boldsymbol{\phi}_n \end{bmatrix} \tag{2.7}$$

and the matrix of eigenvalues is

$$\boldsymbol{\Omega}^2 = \begin{bmatrix} \omega_1^2 & & & & \\ & \ddots & & & \\ & & \omega_i^2 & & \\ & & & \ddots & \\ & & & & \omega_n^2 \end{bmatrix} \tag{2.8}$$

The Lanczos numerical procedure realized in Abaqus/Standard 6.7 environment was used for extracting eigenvalues and eigenvectors of the systems, see e.g. Kleiber (1995), Bathe (1996).

The geometry of the numerical models corresponding to the substitute systems were created in preprocessor of Abaqus/CAE 6.7 environment for the purpose of numerical analysis. The meshes of finite elements were generated. They consisted of hexahedral elements. Quadratic shape functions were applied to the finite elements so that each element possessed twenty nodes. Three translational degrees of freedom were established at each node. Full constrained connection was established between components of the model. The grid of finite elements was presented in Fig. 3. The total number of elements in numerical models equaled approximately 400 000 with average element length 0.0015 m. The convergence of spatial discretization was tested for every numerical model using the value of the first and the last eigenfrequency of interest as a function of degrees of freedom. The convergence of the first and the fourth eigenfrequency for the APB model was presented as an example in Fig. 4 and Fig. 5.

2.2. Experimental study

All measurements realized in the experimental study were done by measuring the system for experimental modal analysis. It consisted of signal recorder

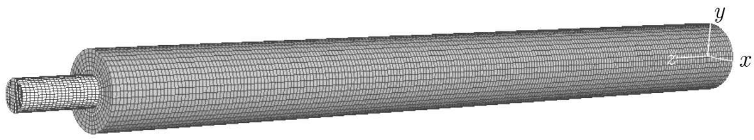

Fig. 3. An example of mesh used in numerical calculations

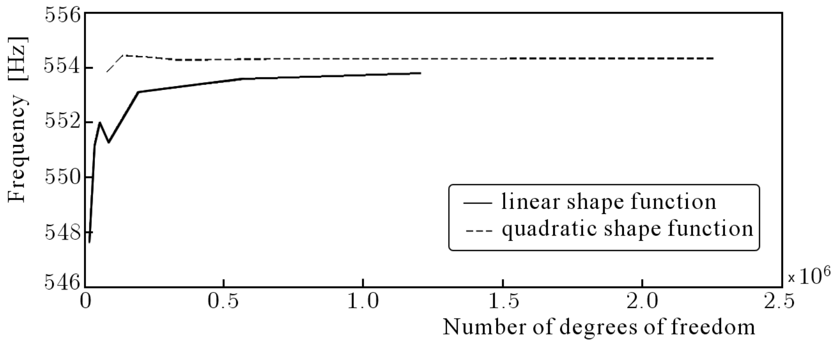

Fig. 4. Convergence of the first eigenfrequency for APB system

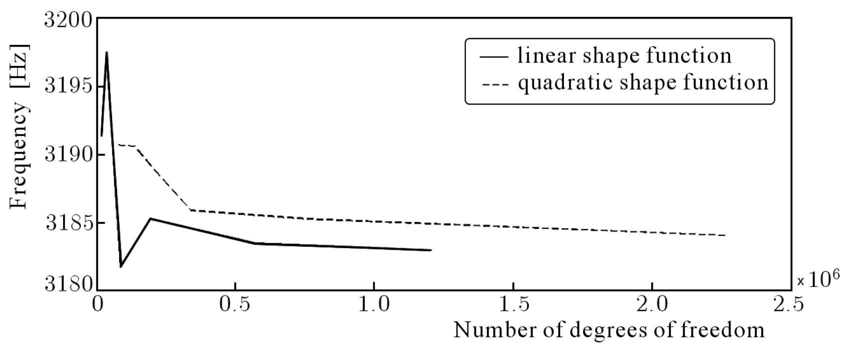

Fig. 5. Convergence of the fourth eigenfrequency for APB system

TEAC RD 135T, two conditioning preamplifiers Bruel&Kjaer 2526, a set of three accelerometers DYTRAN3332 MD, DYTRAN 3143M1, BCM and impact hammer DYTRAN 5800B2. A view of the main components of the measuring system is presented in Fig. 6. The signal recorder was equipped with eight active parallel channels and the sampling rate was set on 24000 Hz. Seven channels were dedicated to the accelerometers and one to the impact hammer. Additionally, the recorder was connected to the PC equipped with DaisyLab environment which allowed for either data storing for subsequent analysis or immediate data processing. Two preamplifires equipped with 4 channels each were responsible for signal conditioning for every single transducer.

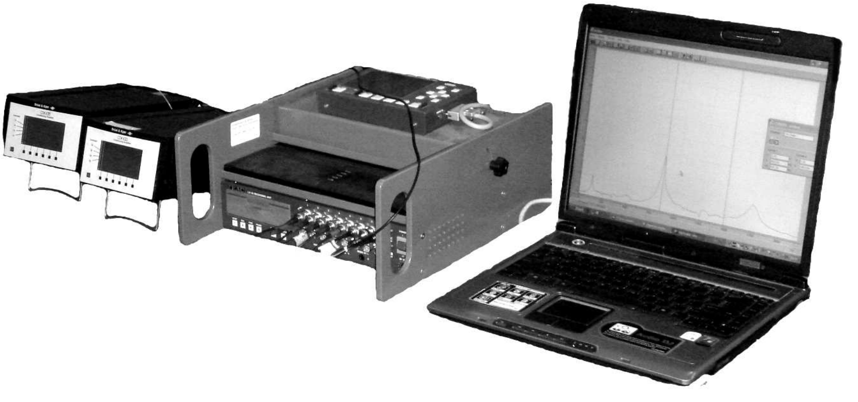

Fig. 6. A view of the main components of the measuring system

Three low mass accelerometers were mounted to the system: two were applied to the circumferential boundary and one to the middle side of the measured system. The accelerometers detected accelerations in function of time. A view of accelerometers arrangement and their orientation in the spatial coordinate system is given in Fig. 7. The measuring axes of transducers were parallel to the direction of excitation. All transducers used in the measurements were fixed to the system by wax. The excitation was generated in the system by an impact hammer equipped with a force sensor to record its time dependence and perform frequency analysis. Three positions of the impact including boundary side, middle side and opposite boundary side were applied in the excitation in a direction parallel to z axis. During the tests every single impact was repeated 9 times. The impacts were separated by a time delay.

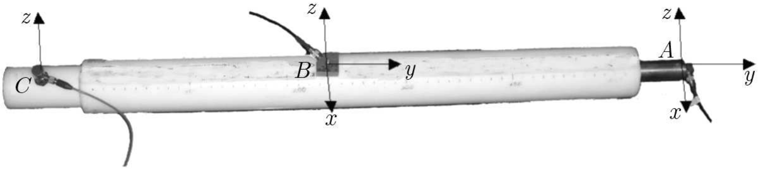

Fig. 7. A view of the accelerometers location

3. Results

3.1. Numerical study

In the numerical study, the eigenfrequencies of considered systems were obtained for APB and PB systems, including data for the first four eigenfrequencies corresponding to bending modes. For each system, three values of the parameter D, namely: $D = 0\%$, $D = 25\%$, $D = 75\%$ were taken into consideration. The eigenfrequencies for the first four modes found for APB and PB systems are presented in Table 2 and Table 3.

Table 2. Eigenfrequenies obtained in numerical analysis for APB system

Mode number	$D = 0\%$	$D = 25\%$	$D = 75\%$
I	553 Hz	520 Hz	249 Hz
II	1378 Hz	916 Hz	677 Hz
III	2282 Hz	1689 Hz	1294 Hz
IV	3182 Hz	2988 Hz	1672 Hz

Table 3. Eigenfrequenies obtained in numerical analysis for PB system

Mode number	$D = 0\%$	$D = 25\%$	$D = 75\%$
I	155 Hz	156 Hz	153 Hz
II	425 Hz	421 Hz	300 Hz
III	808 Hz	776 Hz	458 Hz
IV	1231 Hz	1119 Hz	828 Hz

It can be seen from the analysis of the numerical results that in both systems (APB and PB) all eigenfrequencies are lowered when the deterioration takes place. The eigenfrequency of the first mode shows the smallest changes in the PB system.

3.2. Experimental study

Signals measured from the accelerometer B in the direction parallel to the excitation were taken into consideration. The excitation was parallel to the z axis of the system. The amplitude spectra, which showed resonance frequencies for the considered systems, were obtained from signals recorded in the time domain by using FFT. All data were averaged over 9 realizations of impacts. The values of resonance frequencies for different values of the parameter D

were gathered and presented in Table 4 for the APB system and Table 5 for the PB system.

Table 4. Resonance frequencies obtained experimentally for APB system

Mode number	$D = 0\%$	$D = 25\%$	$D = 75\%$
I	531 Hz	440 Hz	181 Hz
II	1250 Hz	725 Hz	651 Hz
III	1884 Hz	1648 Hz	944 Hz
IV	2900 Hz	2916 Hz	1652 Hz

Table 5. Resonance frequencies obtained experimentally for PB system

Mode number	$D = 0\%$	$D = 25\%$	$D = 75\%$
I	160 Hz	161 Hz	158 Hz
II	440 Hz	439 Hz	285 Hz
III	837 Hz	814 Hz	486 Hz
IV	1238 Hz	1157 Hz	868 Hz

It appears from the results that in both systems under consideration (APB and PB) the resonance frequencies are lowered when the deterioration takes place. The smallest changes can be noticed in the first mode of the PB system.

4. Discussion and conclusions

The comparison of numerical and experimental results shows that when the deterioration between the elements modeling the bone and implant takes place the eigenfrequencies and the resonance frequencies of the systems are lowered. The changes for the APB and PB systems are shown in Fig. 8 and Fig. 9. The predictions of simulations and experimental data are in good qualitative agreement. However in some cases, the values of numerical and experimental results are different from 4% to 21%. This discrepancy may be caused by application of different boundary conditions which were imposed on the system. Since in the numerical study free-free boundary conditions were considered, neither constraints nor fixations of any displacement degree of freedom were applied to the system. In experimental tests it was nesessery to support the system by elastic strips which introduced additional stiffness to the system. The lowest changes of eigenfrequencies and resonance frequencies appear for the first mode especially in the PB system. The highest changes occur at higher mode shapes and amount up to 55% for the APB and 44% for the PB system.

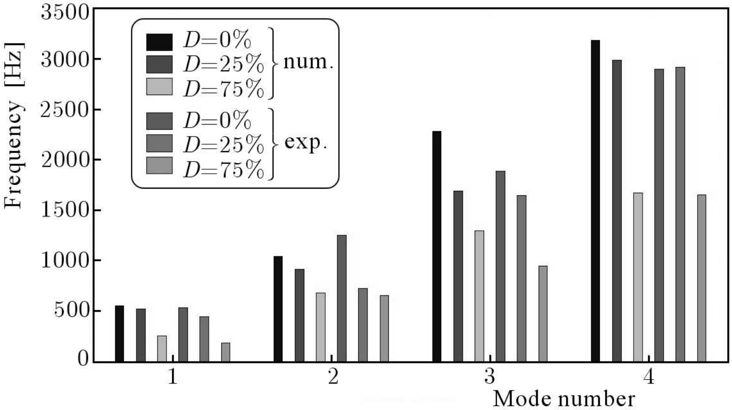

Fig. 8. A comparison of numerical and experimental results for APB system

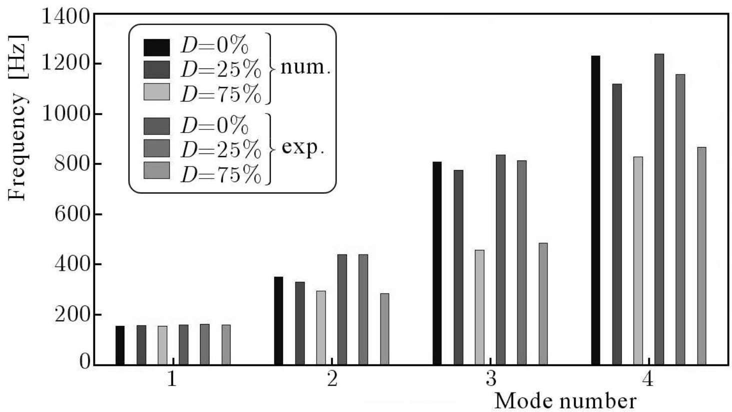

Fig. 9. A comparison of numerical and experimental results for PB system

The results are promising for developing vibrational techniques applied in detecting implant stability, which may be proceeded by appropriate numerical simulations. Eigenfrequencies or resonance frequencies can be used to monitor changes in integrity of the substitute system simulating the implanted bone. Though substitute systems considered in this study are different from real implanted bones, it can be noticed that their numerical simulations and experimental testing create a good starting point for developing vibrational techniques applied to detection of quality of implant systems.

References

1. Bathe K.J., 1996, *Finite Element Procedures*, Inc, Upper Saddle River, New Jersey, The United States of America, Prentice-Hall

2. Georgiou A.P., Cunningham J.L., 2001, Accurate diagnosis of hip prosthesis loosening using a vibrational technique, *Clinical Biomechanics*, **16**, 4, 315-323

3. Keener J.D., Callaghan J.J., 2003, Twenty-five-year results after charnley total arthroplasty in patients less then fifty years old, *Journal of Bone and Joint Surgery*, **85**, 6, 1066-1072

4. Kleiber M., 1995, *Komputerowe metody mechaniki ciał stałych*, Wydawnictwo Naukowe PWN, Warszawa

5. Lieberman K.W., Huo M.H., Schneider R., Salvati E.A., Rodi S., 1993, Evaluation of painful hip arthoplasties. Are technetium bone scans necessary?, *Journal of Bone and Joint Surgery*, **75**, 1, 475-478

6. O'Niell D.A., Harris W.H., 1984, Failed total hip replacement assessment by plain radiographs, arthograms and aspiration of the hip joint, *Journal of Bone and Joint Surgery*, **66**, 1, 540-546

7. Phillips W.C., Kattapuram S.V., 1982, Prosthetic hip replacements: plain films and arthography for component loosening, *American Journal of Radiography*, **138**, 1, 677-682

8. Qi G., Mouchon W.P., Tan T.E., 2003, How much can a vibrational diagnostic tool reveal in total hip arthoplasty loosening, *Clinical Biomechanics*, **18**, 444-458

9. Rosenstein A.D., McCoy G.F., Bulstrode C.J., McLardy-Smith P.D., Cunningham J.L., Turner- Smith A.R., 1989, The differentiation of loose and secure femoral implants in total hip replacement using a vibrational technique: an anatomical and pilot clinical study, *Journal of Engineering in Medicine*, **203**, 2, 77-81

10. Zienkiewicz O.C., Taylor R.L., 2001, The Finite Element Method, Vol. 1, Oxford, England, Butterworth

11. Zilkens K.W., Wicke A., Zilkens J., Bull U., 1998, Nuclear imaging in loosening of hip endoprosthesis, *Z. Orthop. Ihre Grenzgeb.*, **135**, 1, 39-43

Dynamika układów zastępczych połączenia kość-implabt. Badania numeryczne i eksperymentalne

Streszczenie

W pracy przedstawiono badania układów zastępczych zaimplantowanej kości udowej, które dotyczą rozwijania nowych metod diagnostycznych opartych na technikach drganiowych. Wyznaczono zbiory parametrów dynamicznych układów w postaci częstotliwości własnych i rezonansowych dla badań numerycznych i eksperymentalnych. Zmiany parametrów dynamicznych przedyskutowane zostały w kontekście odspajania implantu od kości. Porównano także wyniki badań numerycznych i eksperymentalnych oraz przeanalizowano możliwości zastosowania tej metody w układach anatomicznych.

Manuscript received March 4, 2009; accepted for print April 6, 2009